Available online at www.sciencedirect.com
ScienceDirect
Journal of Power Sources 175 (2008) 244–249
JOURNAL OF POWER SOURCES
www.elsevier.com/locate/jpowsour

Short communication

Comparison of the electrochemical oxidation of borohydride and dimethylamine borane on platinum electrodes: Implication for direct fuel cells

J.I. Martins [a,*], M.C. Nunes [b]

[a] *Departamento de Engenharia Química, FEUP, Rua Roberto Frias, 4200-465 Porto, Portugal*
[b] *Departamento de Engenharia Electrotécnica, Laboratório de Electroquímica, FEUP, Rua Roberto Frias, 4200-465 Porto, Portugal*

Received 27 March 2007; received in revised form 28 July 2007; accepted 5 September 2007
Available online 15 September 2007

Abstract

The electrochemical behaviour of dimethylamine borane and borohydride on platinum electrodes was investigated by cyclic voltammetry and polarization curves in discharges processes. Several overlapping peaks appear in the domain of hydrogen oxidation, i.e., in the potential range of −1.25 V to −0.50 V versus Ag/AgCl, mainly with the borohydride. This behaviour is associated with the hydrolysis of BH_4^- or $(CH_3)_2NHBH_3$. As a consequence of secondary reactions the borohydride and dimethylamine borane oxidation in 3 M NaOH solution shows, respectively, a four- to six-electron process and a four- to five-electron process in direct fuel cells. The direct oxidation of the borohydride exhibits a peak at about −0.07 V versus Ag/AgCl, while the dimethylamine borane peak is at about −0.03 V versus Ag/AgCl. For the 0.04 M concentration the borohydride displays a power density of 31 W m^{-2} which is 16% higher than that of the dimethylamine borane.

Keywords: Borohydride; Dimethylamine borane; Fuel cell; Electrocatalysis; Hydrogen evolution

1. Introduction

The electricity generated by the proton-exchange-membrane (PEM) fuel cells combine the pure hydrogen fuel and the oxygen from air with an energy efficiency that is twice that of the internal-combustion engines. The exhausted products are only water vapour and heat. However, this technology has problems related with the hydrogen storage, because the reduction of its volume by pressure obliges to complexes structures containing multiple layers for hydrogen confinement with inconvenience of rupture strength, and impact resistance. For comparison, a mere 8.2 l of gasoline carries the same energy that 1 kg of hydrogen (146 MJ), which at 150 atm occupies a volume of 91.2 l [1].

The hydrogen can be chemically bound and stored under suitable conditions of temperature and pressure as a solid-hydride compound. The sodium borohydride is a nonreversible hydride that releases hydrogen by hydrolysis and forms metaborate ($NaBO_2$):

$$BH_4^- + 2H_2O \rightarrow BO_2^- + 4H_2 \quad (1)$$

In a PEM fuel cell the delivered hydrogen may produce clean energy for transportation and personal electronics applications where low system weight and portability are important, displaying two electrons according to the following reactions:

$$H_2 \rightarrow 2H^+ + 2e \quad \text{at the anode} \quad (2)$$

$$H_2O + \tfrac{1}{2}O_2 + 2e \rightarrow 2OH^-,\ E^0 = 0.401\ \text{V} \quad \text{at the cathode} \quad (3)$$

In this case it is useful to control directly the storage of the amounts of H_2 produced, i.e., to control the rate of the hydrolysis reaction. This management depends on the catalyst [2,3], solution volume, concentration, and temperature. Amendola et al. [4] using Ru catalysts on the exchange resins have controled the contact time between the catalyst and the borohydride solution,

* Corresponding author. Tel.: +351 225081643; fax: +351 225081449.
E-mail address: jipm@fe.up.pt (J.I. Martins).

0378-7753/$ – see front matter © 2007 Elsevier B.V. All rights reserved.
doi:10.1016/j.jpowsour.2007.09.028

and developed a device generating 1 l H_2 min^{-1} equivalent to a 100 W fuel cell. Kojima et al. [5] have constructed a hydrogen generator using Pt–$LiCoO_2$-coated honeycomb monolith producing 120 nl min^{-1} of H_2 equivalent to 12 kW in a standard PEM fuel cell operating at 0.7 V. But, when the $NaBH_4$ is applied in direct fuel cells (DBFC) [6,7] the wished anodic reaction is characterized by an eight-electron process [8] producing water and metaborate:

$$BH_4^- + 8OH^- \rightarrow BO_2^- + 6H_2O + 8e^-, \quad E^0 = -1.24\,V \tag{4}$$

The overall reaction is the sum of the reactions (3) and (4):

$$BH_4^- + 2O_2 \rightarrow BO_2^- + 2H_2O, \quad E^0 = 1.64\,V \tag{5}$$

This cell has a theoretical standard cell voltage 0.4 V larger than the one of the PEMFC or DMFC. However, secondary reactions such as hydrolysis in several steps [9,10] may occur at some extent, mainly in the solutions at pH < 7, at elevated temperatures or for concentration ratios $[OH^-]/[BH_4^-]$ below 4.4. Thus, the electrochemical oxidation of borohydride [11] and dimethylamine borane [12,13] is a complicated stepwise process that can reduce their expected theoretical performance in direct fuel cells. Based on all the available information on this subject we suggest the following possible initial steps for the anodic behaviour of borohydride ion or dimethylamine borane on platinum electrode:

$$BH_4^- + H_2O \rightarrow BH_3OH^- + 2H^*, \quad \text{chemical step} \tag{6a}$$

$$BH_4^- + OH^- \rightarrow BH_3OH^- + H^* + e^-, \text{electrochemical step} \tag{6b}$$

$$(CH_3)_2NHBH_3 + OH^- \rightarrow (CH_3)_2NH + BH_3OH^-, \quad \text{chemical step} \tag{6c}$$

$$(CH_3)_2NHBH_3 + 2OH^- \rightarrow (CH_3)_2NH + BH_2OH_2^- + H^* + e, \quad \text{electrochemical step} \tag{6d}$$

The oxidation of BH_3OH^- or $BH_2OH_2^-$ to $B(OH)_4^-$ proceeds now through a stepwise transfer of single electrons and radical hydrogen according to the following reactions:

$$BH_3OH^- + OH^- \rightarrow BH_2(OH)_2^- + H^* + e^- \tag{7}$$

$$BH_2(OH)_2^- + OH^- \rightarrow BH(OH)_3^- + H^* + e^- \tag{8}$$

$$BH(OH)_3^- + OH^- \rightarrow B(OH)_4^- + H^* + e^- \tag{9}$$

$$B(OH)_4^- \rightarrow BO_2^- + 2H_2O \tag{10}$$

The produced radical hydrogen may be delivered as hydrogen or oxidized to water.

$$H^* + H^* \rightarrow H_2 \tag{11}$$

$$H^* + OH^- \rightarrow H_2O + e^- \tag{12}$$

In the case of gas liberation, the overall reaction for the borohydride or dimethylamine borane oxidation shows, respectively, a four-electron or three-electron process. This means a decrease of 50% in their specific energy content.

$$BH_4^- + 4OH^- \rightarrow BO_2^- + 2H_2O + 2H_2 + 4e^- \tag{13}$$

$$(CH_3)_2NHBH_3 + 4OH^- \rightarrow BO_2^- + \tfrac{3}{2}H_2 + 2H_2O + (CH_3)_2NH + 3e \tag{14}$$

The number of electrons released by BH_4^- or $(CH_3)_2NHBH_3$ is closely dependent on the nature of the working electrode, and sometimes also with the concentration of fuel. In the case of borohydride, 4e on nickel [6], 4e to 6e on palladium [14], 7e on gold [15], and 2e to 4e on platinum [6], while for dimethylamine borane Sadik et al. [16] have found 1.2e to 2.8e on Au.

The main goal of this work is to compare the electrochemical oxidation of borohydride and dimethylamine borane on platinum electrodes, and to analyse their performance in direct fuel cells.

2. Experimental details

All reagents were of analytical grade and purchased from Aldrich: sodium tetrahydridoborate ($NaBH_4$, 99%), dimethylamine borane ($(CH_3)_2NHBH_3$, 99.99%), ethanol (C_2H_5OH, 99.5%), and sodium hydroxide (NaOH, 97%). The water was distilled twice before use.

2.1. Polarization curves

The electrochemical experiments in 3.0 M NaOH solutions were performed in a one-compartment cell with three electrodes connected to Autolab model PGSTAT20 potentiostat/galvanostat with pilot integration controlled by GPES 4.4 software. Platinum has been used as auxiliary electrode and Ag/AgCl (0.1 M in KCl) as reference electrode. The working sample was a platinum (99.9%) rod, which has been polished with 1 μm diamond paste followed by 0.05 μm alumina. The samples before trials have been clean in baths of water and ethanol provided with ultra-sounds, let sit for about 15 min in solution to stabilize the open circuit potential and finally polarized by applying a determined scan rate.

2.2. Discharge tests

The experiments were carried out in a rectangular plastic beaker containing an anode at the bottom. The cathode is attached to the bottom of a hollow plastic rectangle, which fits into the plastic beaker. The design of our kit-cell is similar to the mini-fuel cell (FC01) of Electro-Chem-Technic and to that proposed by Verma and Basu [17]. A commercial anode of a Pt–carbon-PTFE catalyst (1.0 mg cm^{-2}) on Ni-mesh (EL06,

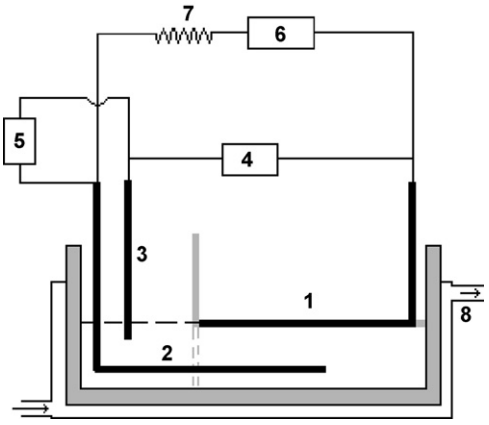

Fig. 1. Scheme of the discharge experiments in the kit-cell monitoring along the time the cell voltage, cell current, and the anode potential: 1, cathode; 2, anode; 3, reference electrode; 4, acquisition cell voltage; 5, acquisition anode potential; 6, acquisition current cell; 7, resistance 5 Ω; 8, control heating system.

Electro-Chem-Technic) and cathode of MnO_2-PTFE on Ni-mesh (EL02, Electro-Chem-Technic) were used. The cathode has been placed at a distance of 1 cm from the anode. The choice for an undivided cell comes from the knowledge that MnO_2 surface does not catalyse the BH_4^- hydrolysis [18].

Cell voltage versus current intensity response was measured galvanostatically by incrementally increasing the current from open circuit and measuring the cell potential, and then reducing the current incrementally again and measuring the cell voltage.

The discharge experiments monitoring at that time were conducted at room temperature using a resistance of 5 Ω, Fig. 1. Multimeters having internal impedance higher than 1 GΩ were connected to register the electrical parameters of voltage cell, current cell, and anode potential. The volume of added electrolyte, a borohydride or dimethylamine borane solution in 3 M sodium hydroxide, closed the electric circuit without submerging the cathode electrode.

2.3. Data treatment

The fuel cell efficiency was determined experimentally by comparing the $NaBH_4$ or $(CH_3)_2NHBH_3$ consumption and the total charge that crosses the electric system. So, the number of electrons liberated during the discharge process was evaluated by the following equation:

$$x = \frac{QM}{Fm} \tag{15}$$

with

$$Q = \int i\,\mathrm{d}t \tag{16}$$

where x is the number of electrons delivered, Q the total charge that cross the electric system (C), F the constant of Faraday (C mol^{-1}), M the molecular weight of $NaBH_4$ or $(CH_3)_2NHBH_3$ (g), m the weighted mass of $NaBH_4$ or $(CH_3)_2NHBH_3$ (g), i the current in the system (A), and t is the time (s).

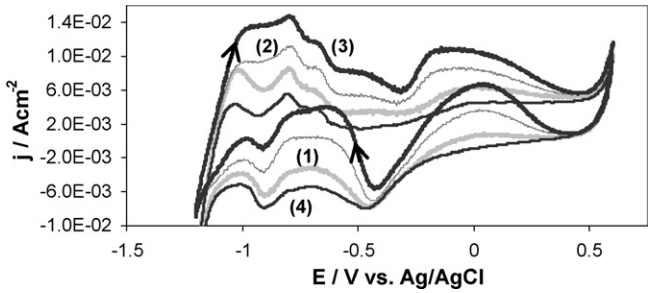

Fig. 2. Tenth scan of cyclic voltammograms of different concentrations of BH_4^- in 3 M NaOH on a Pt rod electrode at 25 °C and scan rate 1000 mV s^{-1}. Legend—(1) 1.323×10^{-2} M; (2) 2.646×10^{-2} M; (3) 3.969×10^{-2} M; (4) 3 M NaOH without BH_4^-.

3. Results and discussion

3.1. Cyclic voltammetry of BH_4^- on Pt

Cyclic voltammograms of the tenth scan from −1.2 V to 0.6 V versus Ag/AgCl at 1000 mV s^{-1} on platinum electrode for different concentrations of BH_4^- in 3 M NaOH medium are presented in Fig. 2. The recorded j–E curves are complex and characterized by several oxidation and reduction peaks. The blank solution (3 M NaOH) voltammogram presents three oxidation peaks, respectively, at −1.03 V, −0.78 V, and −0.65 V, which are related to the ionization of hydrogen bonded to platinum and produced by the cathodic discharge of water [19–25]. We deduce by the analysis of voltammograms with BH_4^- that the oxidation current of the whole voltammogram increases with its concentration, and in particularly the current density of those peaks. Moreover, the first peak is shifted to more positive potentials with the scan rate, (Fig. 3a), and the ratio ($j_{p,a}/v^{1/2}$) form for the second scan, to avoid the holding of hydride species generated at low potentials in the first scan, decreases, Table 1. These results indicate a CE mechanism [26], i.e., the hydrolysis of BH_4^- (reaction (6a)) followed by the hydrogen ionization (reaction (12)). This conclusion is in line with the observations of Gyenge [27]. It is remarked that the first three peaks are not discernible at low scan rates, (Fig. 3b).

Table 1
Current density of the first peak observed in the second scan of the voltammograms obtained on Pt rod at 25 °C using different scan rates for $NaBH_4$ 1.323×10^{-3} M and $(CH_3)_2NHBH_3$ 2.646×10^{-3} M in 3 M NaOH

Compound	Scan rate, v (mV^{-1} s^{-1})	j_p (1st peak) (mA cm^{-2})	$j_p v^{-1/2}$ (mA cm^{-2} mV$^{-1/2}$)
$NaBH_4$	25	2.45	0.490
	100	4.19	0.419
	1000	8.74	0.276
	1200	9.15	0.264
$(CH_3)_2NHBH_3$	2	0.699	0.494
	5	1.08	0.483
	10	1.44	0.455
	25	2.16	0.432
	100	4.27	0.427
	1000	12.5	0.395
	1200	13.1	0.378

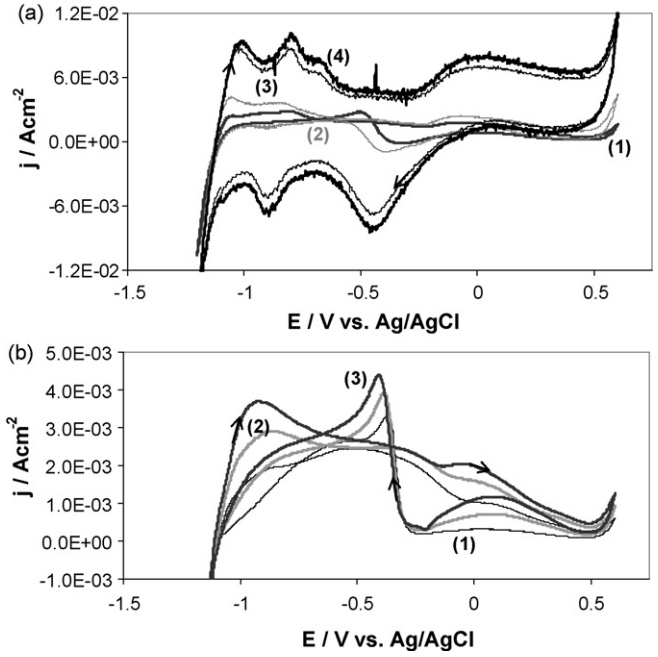

Fig. 3. Second scan of cyclic voltammograms of 1.323×10^{-2} M BH_4^- in 3 M NaOH on a Pt rod at 25 °C. Legend—(a): (1) 25 mV s^{-1}; (2) 100 mV s^{-1}; (3) 1000 mV s^{-1}; (4) 1200 mV s^{-1}; (b): (1) 2 mV s^{-1}; (2) 5 mV s^{-1}; (3) 10 mV s^{-1}.

An oxidation wave appears in the potential range between −0.62 V and −0.30 V. In order to clarify this observation we have performed additional polarization experiments, thereby reducing the sweeping domain. The voltammogram obtained over the potential range −1.2 to 0.35 V (Fig. 4a) shows an anodic peak at −0.60 V in the forward scan; also, in the reverse scan another anodic peak appears at −0.42 V. We associate both peaks with the BH_3OH^- direct oxidation according to the reactions (18a) or (18b).

$$BH_3OH^- + 3OH^- \rightarrow BO_2^- + \tfrac{3}{2}H_2 + 2H_2O + 3e^- \quad (18a)$$

$$BH_3OH^- + 3OH^- \rightarrow BO_2^- + 3H^+ + 2H_2O + 6e^- \quad (18b)$$

We may considerer that reaction (18b) results from the addition of reactions (19) and (10).

$$BH_3(OH)^- + 3OH^- \rightarrow B(OH)_4^- + 3H^+ + 6e^- \quad (19)$$

Okinaka [28] observed a similar wave between −0.67 V and −0.30 V (on Au in 0.2 M KOH), Gyenge [27] between −0.45 V and −0.20 V versus Ag/AgCl (on Pt 2 M NaOH), Zhang et al. [29] at about −0.38 V versus SCE (on Au in 2 M NaOH), and Gardiner and Collat [10] from polarography studies reported a half-wave potential at −0.64 V versus SCE (on Hg in 0.001 M NaOH).

At more positive potentials in the forward scan a broad anodic peak at about −0.13 V appears which increases proportionally to the content of BH_4^- in the solution, and in the reverse scan an anodic wave between −0.20 V and 0.50 V appears. The peak has been refined to the potential at about −0.07 V by scanning the potential between −0.35 V and 0.60 V (Fig. 4b). This peak and the anodic wave in the backward scan are associated with the BH_4^- direct oxidation. It has been reported by Okinava [28]

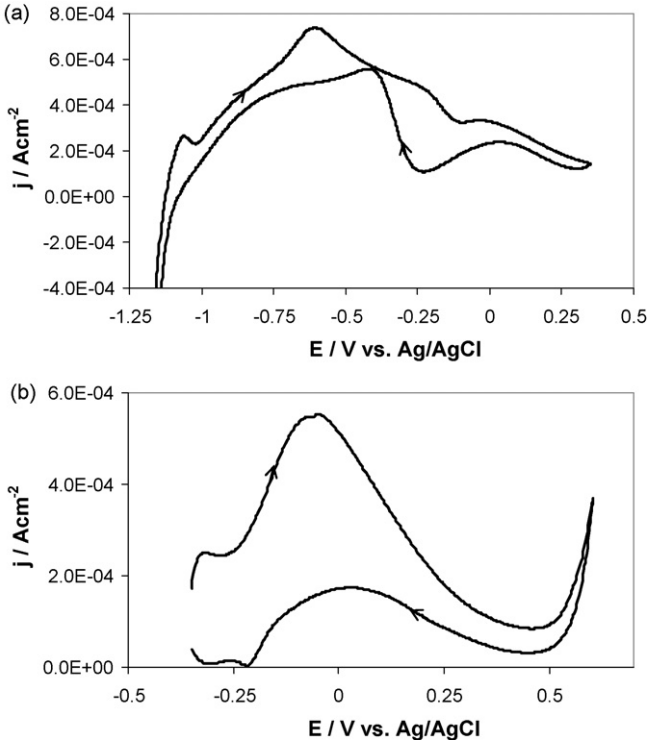

Fig. 4. Second scan of cyclic voltammograms of 1.323×10^{-2} M BH_4^- in 3 M NaOH on a Pt rod at 25 °C and 25 mV s^{-1}. Scanning the potential between: (a) −1.2 V and 0.35 V; (b) −0.35 V and 0.60 V.

that the direct oxidation of BH_4^- occurs between −0.20 V and −0.05 V on Au in 0.2 M KOH, while Gyenge [27] obtained a peak between −0.15 V and −0.05 V on Pt in 2 M NaOH.

3.2. Cyclic voltammetry of $(CH_3)_2NHBH_3$ on Pt

Fig. 5 shows the effect of $(CH_3)_2NHBH_3$ concentration on the relation *j–E*, which are quite different of those obtained for BH_4^-. In the forward scan a peak at −1.03 V is observed, a wide anodic wave until about −0.6 V disclosing a broad peak centred at about −0.75 V, and a second large anodic wave defining a broad peak at about −0.03 V. The effect of scan rate on the electrooxidation of $(CH_3)_2NHBH_3$ is presented in Fig. 6. At low scan rates beyond the first peak and the peak at −0.03 V, a new anodic peak at about −0.42 V appears in the reverse scan associated

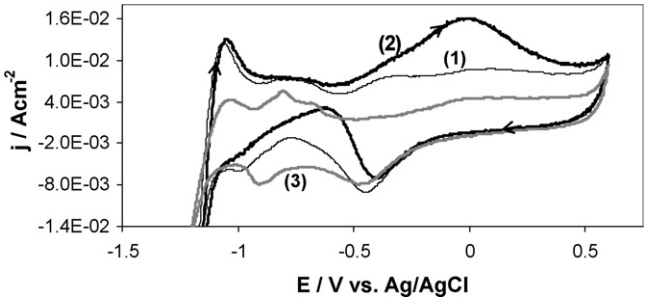

Fig. 5. Tenth scan of cyclic voltammograms of different concentrations of $(CH_3)_2NHBH_3$ in 3 M NaOH on a Pt rod electrode at 25 °C and scan rate 1000 mV s^{-1}. Legend: (1) 1.323×10^{-2} M; (2) 2.646×10^{-2} M; (3) 3 M NaOH without $(CH_3)_2NHBH_3$.

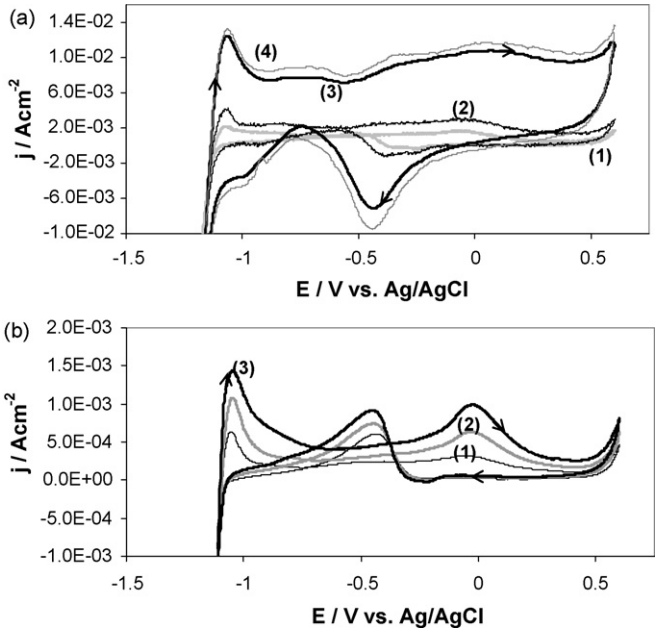

Fig. 6. Second scan of cyclic voltammograms of 2.646×10^{-2} M $(CH_3)_2NHBH_3$ in 3 M NaOH on a Pt rod at 25 °C. Legend—(a): (1) 25 mV s^{-1}; (2) 100 mV s^{-1}; (3) 1000 mV s^{-1}; (4) 1200 mV s^{-1}; (b): (1) 2 mV s^{-1}; (2) 5 mV s^{-1}; (3) 10 mV s^{-1}.

with the BH_3OH^-, and the intermediates species (formed during the stepwise mechanism) adsorbed on the platinum surface. The first peak shifts to more positive potentials with the scan rate, and the ratio ($j_{p,a}/v^{1/2}$) decreases, Table 1. These results indicate a CE mechanism [26], i.e., the chemical reaction (6c) followed by electrochemical reaction (12) [19]. The first wide anodic wave is mainly related with the BH_3OH^- direct oxidation according to the reaction (18a), while the peak at about −0.02 V is related with reaction (18b).

3.3. Discharge curves of BH_4^- and $(CH_3)_2NHBH_3$ in direct fuel cell

Fig. 7 shows the kit-cell polarization behaviour at 25 °C for 0.04 M concentration of borohydride or dimethylamine borane in 3 M NaOH medium. The open circuit voltage of

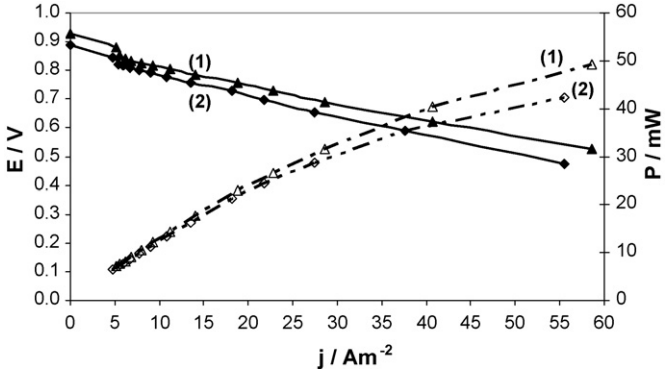

Fig. 7. Cell voltage and power density vs. current density for the kit-cell at 25 °C using a fuel concentration of 0.04 M in 3 M NaOH: Curve (1) for BH_4^- and curve (2) for $(CH_3)_2NHBH_3$.

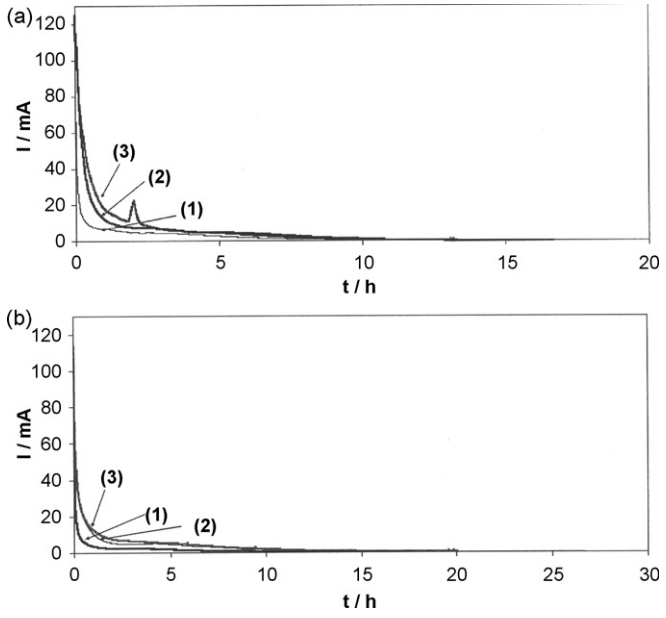

Fig. 8. Discharge curves with different concentrations of (a) BH_4^- and (b) $(CH_3)_2NHBH_3$ in direct kit-cell (20 ml) in 3 M NaOH at 25 °C: (1) 1.323×10^{-2} M; (2) 2.646×10^{-2} M; (3) 3.969×10^{-2} M.

the cell using the BH_4^- is slightly higher than that using $(CH_3)_2NHBH_3$. Although the OCVs are slightly higher than that observed in a hydrogen fuel cell, they were significantly lower than the theoretical expected values. A further investigation has shown that the system initially presents an anode potential of about −0.75 V versus NHE and a cathode potential of 0.18 V versus NHE. The drop in the open circuit potential of the anode may be associated to the complex anodic mechanism of borohydride oxidation composed by several intermediates. In the case of the cathode it is mainly caused by the overpotential for the oxygen reduction. A linear relation in almost the entire current density range characterizes the polarization curves of the kit-cell for both fuels. However, the final voltage loss is attributed to the concentration overpotential. The dimethylamine borane kit-cell displays a maximum power density of 26 W m^{-2}, about 16% lower than the value of 31 W m^{-2} observed for borohydride. It should be referred that increasing the distance between the cathode and anode from 1 cm to 2 cm results in a decrease of about 10% in the cell power.

Fig. 8 shows the discharge curves in the direct kit-cell (fuel volume 20 ml) for several amounts of BH_4^- and $(CH_3)_2NHBH_3$ in 3 M NaOH medium at 25 °C. Table 2 summarizes the number of electrons disclosed on the experiments and obtained by

Table 2
Number of electrons disclosed in discharges at 25 °C using the kit-cell for different concentration of borohydride and dimethylamine borane

Fuel	Fuel concentration (M)		
	1.323×10^{-2}	2.646×10^{-2}	3.969×10^{-2}
BH_4^-	5.34	5.68	4.32
$(CH_3)_2NHBH_3$	3.86	4.68	3.76

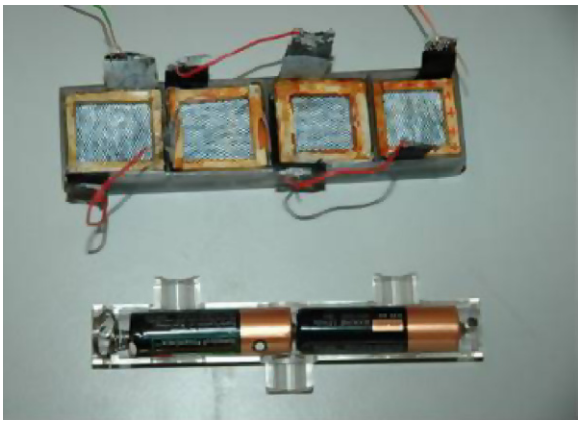

Fig. 9. Comparison of the kit-cell disclosing a cell voltage of 3.5 V with a system of two commercial piles of 1.5 V.

integrating the current along the time through Eq. (16) and substituting in Eq. (15). These results show the presence of hydrolysis for both fuels, and in agreement with the analysis performed on cyclic voltammetry data, i.e., a complex stepwise oxidation process with the hydrogen evolution. The hydrolysis depends on fuel concentration and is more accentuated for borohydride. Indeed, for the considered fuel concentrations it is possible to deduce that the number of electrons disclosed by dimethylamine borane is lesser 27%, 18% and 13% than borohydride, respectively, for concentrations 1.323×10^{-2} M, 2.646×10^{-2} M, and 3.969×10^{-2} M. Without the hydrolysis the dimethylamine borane should disclose theoretically lesser 25% of electrons than borohydride. In a previous work we have shown that a conveyable $SC(NH)_2/BH_4^-$ concentration ratio of 0.6 inhibits borohydride hydrolysis allowing direct BH_4^- oxidation in an eight-electron process [30].

3.4. Development of a kit-cell displaying a cell voltage of 3.5 V

We have built a kit-cell (Fig. 9a) composed by four cells in series, having each one an area of 12 cm^2 and a capacity of 7.5 ml. The kit-cell with a solution of 30 mg of borohydride in 30 ml of 3 M NaOH has presented an open cell voltage of 3.5 V and a maximum power density of 125 W m^{-2} for a current density of 6.25 mA cm^{-2}. This kit-cell with 120 mg of borohydride in 30 ml of NaOH has been applied to a radio (with an output power of 10 mW) that has worked for about 3 h.

4. Conclusions

The electrochemical oxidation of borohydride and dimethylamine borane on platinum in alkaline medium 3 M NaOH occurs according to a complex mechanism associated to catalytic hydrolysis and direct oxidation of BH_4^- or $(CH_3)_2NHBH_3$ at potentials over −0.20 V versus Ag/AgCl. The discharges experiments show for borohydride oxidation a four- to six-electron process and for dimethylamine borane a four- to five-electron process.

References

[1] F.E. Pinkerton, B.G. Wicke, Industrial Physicist 10 (2004) 20.
[2] A. Levy, J.B. Brown, C.J. Lyons, Ind. Chem. Eng. 52 (1960) 211.
[3] C.M. Kaufman, B. Sen, J. Chem. Soc., Dalton Trans. 307 (1985).
[4] S.C. Amendola, S.L. Sharp-Goldman, M.S. Janjua, M.T. Kelly, P.J. Petillo, M. Binder, J. Power Sources 85 (2000) 186.
[5] Y. Kojima, K. Ken-Ichirou Suzuki, Y. Fukumoto, M. Kawai, H. Kimbara, S. Nakanishi, Matsumoto, J. Power Sources 125 (2004) 22.
[6] M.E. Indigo, R.N. Snyder, J. Electrochem. Soc. 109 (1962) 1104.
[7] R. Jasinski, Electrochem. Technol. 3 (1965) 40.
[8] W.H. Stockmayer, D.W. Rice, C.C. Stephenson, J. Am. Chem. Soc. 77 (1955) 1980.
[9] J.A. Gardiner, J.W. Collat, J. Am. Chem. Soc. 87 (1965) 1692.
[10] J.A. Gardiner, J.W. Collat, Inorg. Chem. Soc. 4 (1965) 1208.
[11] J.P. Helder, A. Hickling, Trans. Faraday Soc. 58 (1962) 1852.
[12] T. Homma, A. Tamaki, H. Nakai, T. Osaka, J. Electroanal. Chem. 559 (2003) 131.
[13] T. Homma, H. Nakai, M. Onishi, T. Osaka, J. Phys. Chem. 103 (1999) 1774.
[14] B.H. Liu, Z.P. Li, S. Suda, Electrochim. Acta 49 (2004) 3097.
[15] S.C. Amendola, P. Onnerud, M.T. Nelly, P.J. Petillo, S.L. Sharp-Goldman, M. Binder, J. Power Sources 84 (1999) 130.
[16] O.A. Sadik, H. Xu, A. Sargent, J. Electroanal. Chem. 583 (2005) 167.
[17] A. Verma, S. Basu, J. Power Sources 145 (2005) 282.
[18] R.X. Feng, H. Dong, Y.D. Wang, X.P. Ai, Y.L. Cao, H.X. Yang, Electrochem. Commun. 7 (2005) 449.
[19] J.O'M. Bockris, Modern Aspects of Electrochemistry, vol. 1, Butterworths, 1954, p. 141 (Chapter 3).
[20] M. Breiter, W. Volkl, Z. Electrochem. 59 (1955) 681.
[21] M. Breiter, C.A. Knorr, R. Meggle, Z. Electrochem. 59 (1955) 153.
[22] M. Breiter, H. Kammermaier, C.A. Knorr, Z. Electrochem. 60 (1956), 37,119,454.
[23] B.E. Conway, L. Bai, J. Electroanal. Chem. 198 (1986) 149.
[24] A. Bewick, A.M. Tuxford, J. Electroanal. Chem. 47 (1973) 255.
[25] A. Bewick, K. Kunimatsu, J. Robinson, J.W. Russell, J. Electroanal. Chem. 119 (1981) 175.
[26] R. Greef, R. Peat, L.M. Peter, D. Pletcher, J. Robinson, Instrumental Methods in Electrochemistry, Ellis Horwood, 1993, pp. 187–188 (Chapter 6).
[27] E. Gyenge, Electrochim. Acta 49 (2004) 965.
[28] Y. Okinaka, J. Electrochem. Soc. 120 (1973) 739.
[29] X.-B. Zhang, S. Han, J.-M. Yan, M. Chandra, H. Shioyama, K. Yasuda, N. Kuriyama, T. Kobayashi, Q. Xu, J. Power Sources 168 (2007) 167.
[30] J.I. Martins, M.C. Nunes, R. Koch, L. Martins, M. Bazzaoui, Electrochim. Acta 52 (2007) 6443.